Biochemical Pharmacology 177 (2020) 113941

Contents lists available at ScienceDirect

Biochemical Pharmacology

journal homepage: www.elsevier.com/locate/biochempharm

Src-family kinase inhibitors block early steps of caveolin-1-enhanced lung metastasis by melanoma cells

Rina Ortiz[a,b], Jorge Díaz[c,d], Natalia Díaz-Valdivia[c,d], Samuel Martínez[c,d], Layla Simón[c,d], Pamela Contreras[c,d], Lorena Lobos-González[c,e], Simón Guerrero[c,d], Lisette Leyton[c,d,*], Andrew F.G. Quest[c,d,*]

[a] Centro de Biotecnología, Universidad Técnica Federico Santa María, Avenida España 1680, Valparaíso, Chile
[b] Departamento de Física, Universidad Técnica Federico Santa María, Avenida España 1680, Valparaíso, Chile
[c] Cell Communication Laboratory, Center for Studies on Exercise, Metabolism and Cancer (CEMC), Institute of Biomedical Sciences (ICBM), Faculty of Medicine, Universidad de Chile, Santiago, Chile
[d] Advanced Center for Chronic Diseases (ACCDiS), Santiago, Chile
[e] Center for Regenerative Medicine, Faculty of Medicine, Universidad del Desarrollo, Clinica Alemana, Santiago, Chile

ARTICLE INFO

Keywords:
Src-family kinase inhibitors
Phospho-caveolin-1
Migration
Metastasis
Melanoma

ABSTRACT

In advanced stages of cancer disease, caveolin-1 (CAV1) expression increases and correlates with increased migratory and invasive capacity of the respective tumor cells. Previous findings from our laboratory revealed that specific ECM-integrin interactions and tyrosine-14 phosphorylation of CAV1 are required for CAV1-enhanced melanoma cell migration, invasion and metastasis *in vivo*. In this context, CAV1 phosphorylation on tyrosine-14 mediated by non-receptor Src-family tyrosine kinases seems to be important; however, the effect of Src-family kinase inhibitors on CAV1-enhanced metastasis *in vivo* has not been studied. Here, we evaluated the effect of CAV1 and c-Abl overexpression, as well as the use of the Src-family kinase inhibitors, PP2 and dasatinib (more specific for Src/Abl) in lung metastasis of B16F10 melanoma cells. Overexpression of CAV1 and c-Abl enhanced CAV1 phosphorylation and the metastatic potential of the B16F10 murine melanoma cells. Alternatively, treatment with PP2 or dasatinib for 2 h reduced CAV1 tyrosine-14 phosphorylation and levels recovered fully within 12 h of removing the inhibitors. Nonetheless, pre-treatment of cells with these inhibitors for 2 h sufficed to prevent migration, invasion and trans-endothelial migration *in vitro*. Importantly, the transient decrease in CAV1 phosphorylation by these kinase inhibitors prevented early steps of CAV1-enhanced lung metastasis by B16F10 melanoma cells injected into the tail vein of mice. In conclusion, this study underscores the relevance of CAV1 tyrosine-14 phosphorylation by Src-family kinases during the first steps of the metastatic sequence promoted by CAV1. These findings open up potential options for treatment of metastatic tumors in patients in which Src-family kinase activation and CAV1 overexpression favor dissemination of cancer cells to secondary sites.

1. Introduction

Caveolin-1 (CAV1) is an integral membrane protein with several functions under physiological conditions, such as caveolae formation and endocytosis, cholesterol homeostasis and signal transduction [1]. Additionally, the role of this protein in pathological conditions has also been studied [2–4]. Considerable information concerning the role of CAV1 in cancer is available [5–10], however, in conjunction these studies point towards a complex role in the development of the disease [7]. Initially, during tumor development, reduced expression of CAV1 linked to methylation of the promoter region is observed, consistent with its function as a tumor suppressor; however, in advanced stages of the disease, increased levels of the protein correlate with the development of metastasis [8].

Cancer cell metastasis requires the coordinated and directional movement of cells in response to changes in the extracellular microenvironment [11,12]. Specifically, metastatic colonization involves the adhesion of tumor cells in the microvasculature and subsequent cell migration through the endothelium to a secondary site, a process referred to as trans-endothelial migration (TEM) [13], which appears to

* Corresponding authors at: Cell Communication Laboratory, Center for Studies on Exercise, Metabolism and Cancer (CEMC), Institute of Biomedical Sciences (ICBM), Faculty of Medicine, Universidad de Chile, Santiago, Chile.
E-mail addresses: lleyton@med.uchile.cl (L. Leyton), aquest@med.uchile.cl (A.F.G. Quest).

https://doi.org/10.1016/j.bcp.2020.113941
Received 17 January 2020; Accepted 26 March 2020
Available online 30 March 2020
0006-2952/

be comparable to leukocyte diapedesis [14]. CAV1 favors metastasis by promoting cell migration and invasion [15], and elevated CAV1 levels are associated with the progression of different types of cancer, such as breast, prostate [16,17] and colon [6] cancer, as well as melanoma [18]. In prostate cancer, significantly increased levels of CAV1 in tissue and plasma are associated with progression of the disease and poor prognosis of patients [19–21]. Thus, CAV1 can be considered a potential biomarker that may be useful in the development of therapeutic strategies for the treatment of prostate cancer [16]. Similarly, in hepatic carcinoma, elevated levels of CAV1 in patient samples correlate with progression of the disease and are associated with intra hepatic metastasis, a relevant factor in defining patient prognosis [22].

Two variants of CAV1 have been described, CAV1α (aa 1–174) and CAV1β (aa 32–174); the latter is suggested to be generated by either alternative splicing or alternative initiation from the same transcript [23,24]. Common functions have been ascribed to both variants, although differences during development have been detected [25,26]. However, only CAV1α contains the tyrosine-14 (Y14) residue, a target site for phosphorylation by the non-receptor tyrosine kinases, including Src, Fyn, Yes and c-Abl, in response to a large number of stimuli [8,27–29]. In this context, phosphorylation at this site has been widely associated with important events during cell migration, both in normal and tumor cells [9,30–32]. In the latter case, for instance, CAV1 stimulates tumor invasion through Rho activation and FAK stabilization in focal adhesions in a Src-dependent manner [33].

Previously, our group evaluated the metastatic potential of CAV1 in murine melanoma B16F10 cells, which are derived from the C57BL/6 mouse. Overexpression of CAV1 in B16F10 cells increased Rac1 activation and subsequent cell migration *in vitro,* which then translated into a 3-fold increase in lung metastasis *in vivo* [10,31]. The same effects of CAV1 are observed in the human melanoma A375 cell line. Additionally, metastasis in mice is inhibited when the tumor suppressor E-cadherin is introduced into CAV1 expressing cells [10] and this ability of E-cadherin is linked to recruitment of the non-receptor tyrosine phosphatase PTPN14 to the CAV1/E-cadherin complex and CAV1 dephosphorylation [34]. Indeed, our results also indicate that CAV1 requires phosphorylation on Y14 to enhance migration specifically on two abundant ECM substrates in the lung (fibronectin and laminin), as well as invasion, trans-endothelial cell migration and *in vivo* metastasis [31,32]. On the other hand, pharmacological inhibition of Src kinase reduces migration suggesting the requirement of tyrosine-14 phosphorylation for CAV1-enhanced migration [31], however, the effect of this inhibitor on CAV1-enhanced metastasis is unknown. Interestingly, neither the CAV1 mutation Y14F (non-phosphorylatable) nor Y14E (phosphomimetic) affect the ability of the protein to function as a tumor suppressor [32], even in the absence of E-cadherin [10]. Therefore, reducing phosphorylation of CAV1 on Y14 can be viewed as an ideal therapeutic target to diminish metastasis without affecting the beneficial function of the protein as a tumor suppressor.

Thus, the aim of this study was to evaluate the effect of inhibition of CAV1 phosphorylation on migration, invasion and metastasis of melanoma cells. To that end, we used the pharmacological experimental inhibitor of Src-family kinase proteins, named PP2 (4-amino-5- (4-chloro-phenyl) -7- (t-butyl) pyrazolo [1–19,21–79] pyrimidine) [53], as well as the clinically relevant Src/Abl inhibitor, dasatinib (DST) [35,41]. Moreover, we used gold nanoparticles as tracking devices to label B16F10 cells expressing CAV1 [51] and study how treatment of the cells with the inhibitors affected lung metastasis. Our results underscore the relevance of CAV1 phosphorylation on tyrosine-14 in migration and invasion, as well as during the initial steps of lung colonization in mice intravenously injected with B16F10 melanoma cells.

2. Materials and methods

2.1. Antibodies and reagents

Rabbit polyclonal anti-caveolin-1 (Transduction Laboratories, Lexington, KY, USA) and anti-actin (R&D Systems, MN, USA) antibodies, as well as the goat polyclonal anti-MMP-2/9 (Santa Cruz Biotechnology, CA, USA), mouse monoclonal anti-pY14-caveolin-1, anti-Rac1 (Transduction Laboratories) and anti c-Abl (Santa Cruz Biotechnology) antibodies were used as indicated by the manufacturers. Goat anti-rabbit and goat anti-mouse IgG antibodies coupled to horseradish peroxidase (HRP) were from Merck-Millipore (Billerica, MA, USA) and KPL Laboratories (Washington DC, USA), respectively. The ECL chemiluminescent substrate and the BCA protein determination kit were from Pierce (Rockford, IL, USA). Fetal bovine serum (FBS) was from Biological Industries (Cromwell, CT, USA). Cell culture media and antibiotics were from GIBCO (Invitrogen, Carlesbad, CA, USA). PP2 was from Enzo Life Science International (Plymouth Meeting, PA, USA). DST was from Jomar Life Research (Selleckchem, TX, USA). All chemicals were purchased from Sigma-Aldrich (St. Louis, US) unless indicated otherwise.

2.2. Cell culture

Metastatic murine melanoma cells B16F10 (ATCC, #CRL6475, provided by Laurence Zitvogel, Institut Gustav Roussy, Villejuif, France) were cultured in RPMI 1640 medium supplemented with 10% FBS and antibiotics (100 U/mL penicillin and 100 mg/mL streptomycin) and used for all experiments in passage numbers between 9 and 14. EA.hy926 endothelial cells, used in passage numbers between 15 and 25 (ATCC, #CRL2922, kindly donated by Gareth Owen, Pontificia Universidad Católica de Chile) were maintained in IMEM medium supplemented with 10% FBS and antibiotics as mentioned above. Cells were maintained at 37 °C and 5% CO_2.

2.3. Transfection of B16F10 melanoma cells

The plasmids pLacIOP (referred to as mock) and pLacIOP-caveolin-1 (referred to as CAV1, containing the full-length dog caveolin-1 sequence, NCBI Reference Sequence: NP_001003296.1) were previously described [6]. B16F10(mock) and B16F10(CAV1) cells were grown to 50–60% confluence in 6 multi-well plates and then transfected with 2 μg of c-Abl-GFP plasmid, c-Abl–KD-GFP (kinase dead dominant-negative form of c-Abl) plasmid or the empty GFP vector (kindly provided by Dr. Alejandra Alvarez, Pontificia Universidad Católica de Chile, Santiago, Chile).

2.4. Western blotting

B16F10 cells grown to 70–80% confluence, were washed with cold PBS and lysed in 0.2 mM HEPES (pH 7.4) buffer containing 0.1% SDS, phosphatase inhibitors (1 mM Na_3VO_4) and a protease inhibitor cocktail (10 mg/mL benzamidine, 2 mg/mL antipain, 1 mg/mL leupeptin, 1 mM PMSF). Protein concentrations were determined using the BCA method. Total protein extracts (30 μg/lane) were separated by SDS-polyacrylamide gel electrophoresis (SDS-PAGE) and then transferred to a nitrocellulose membrane. Blots were blocked with 5% milk in 0.1% Tween-PBS and then probed for actin (1:5000), caveolin-1 (1:5000), Rac1 (1:3000), c-Abl (1:3000), MMP-2 (1:1000) and MMP-9 (1:1000) with specific antibodies at the indicated dilutions. Alternatively, blots were blocked with 5% gelatin in 0.1% Tween-PBS and probed with anti-pY14-caveolin-1 (1:3000) antibody diluted as indicated in blocking buffer. Bound antibodies were detected with HRP-conjugated secondary goat anti-rabbit or goat anti-mouse antibodies (1:3000) and the ECL system (Thermofisher, MA, USA). To obtain quantitative data, western blots were analyzed using Image J software (NIH, USA). Values

shown for protein expression were averaged from results obtained in three independent experiments.

2.5. Pre-incubation of B16F10 cells with Src-family kinase inhibitors

For all the experiments, B16F10(mock) and B16F10(CAV1) cells where pre-incubated with 10 μM of PP2 or 100 nM of DST for 2 h. Then, cells were washed with PBS, resuspended in culture medium for *in vitro* experiments or physiological saline solution for *in vivo* experiments. The rationale for using these concentrations is based on previous results from our group showing significant effects of 10 μM PP2 in B16F10 migration and CAV1 phosphorylation [31]. On the other hand, 100 nM of DST is sufficient to reduce significantly migration and invasion of human A2058 and 1205-Lu melanoma cells [39] as well as prostate cancer cells [65].

2.6. Transwell migration assay

Migration was assayed in Boyden Chambers (Corning Costar Transwell, 6.5 mm diameter, 8 μm pore size; Costar, Corning, NY, USA) according to the manufacturer's instructions. Briefly, the lower surfaces of the inserts were coated with fibronectin (2 μg/ml). B16F10 cells (5×10^4) pre-treated for 2 h with PP2 or DST, were re-suspended in serum-free medium and then plated in the top of each chamber insert. Serum-free medium was added to the bottom chamber [32]. After 2 h, inserts were removed, washed and cells that migrated to the lower side of the insert membranes were stained with 0.1% crystal violet in 2% ethanol and counted using an inverted microscope. In each independent experiment, six images per condition were evaluated.

2.7. Invasion assay

Assays were performed in matrigel chambers (BD Matrigel invasion chambers, 6.5 mm diameter, 8 μm pore size; Beckton-Dickinson, Franklin Lakes, NJ, USA) according to the manufacturer's instructions. B16F10 cells (5×10^4) pre-treated for 2 h with PP2 or DST, were re-suspended in serum-free medium and then added to the upper section of each chamber insert. Complete medium was added to the bottom chamber. After 22 h, inserts were removed, washed and cells that migrated to the lower side of the insert membranes were stained with toluidine blue in 1% methanol and counted using an inverted microscope. In each independent experiment, six images per condition were evaluated.

2.8. Zymography

B16F10(mock) and B16F10(CAV1) cells induced by IPTG for 48 h were serum-starved for 16 h and then treated with PP2 or vehicle (DMSO) for 2 h. Supernatants of three independent experiments were collected and analyzed by zymography to determine the enzymatic activity of metalloproteinases (MMPs) MMP-2 and MMP-9 using the protocol previously described by Goicovich [50]. Samples were resolved in 10% polyacrylamide gels co-polymerized with gelatin (1 mg/ml). Samples (30 μg protein) were incubated for 30 min in sample buffer (0.4 M Tris-HCl, pH 6.8, containing 5% SDS, 20% glycerol, 0.03% Bromophenol Blue) under non-reducing conditions, at room temperature. After electrophoresis, gels were incubated in 2.5% Triton X-100 for 2 h at room temperature, in order to eliminate residual SDS. Gels were then incubated by 24 h in metalloproteinase test buffer (150 mM Tris-HCl, pH 7.5, 150 mM NaCl, 5 mM CaCl2, 0.02% NaN_3) at 37 °C. Gels were fixed and stained with Coomassie Blue R-250. As a loading control, the same samples were separated on a gel and stained with Coomassie Blue R-250. Degradation of gelatin due to the gelatinase activity of MMP-2 and −9 was quantified by densitometric analysis of the clear bands in the zymography gels using the Image J software (NIH, USA) and normalized to the respective loading controls.

2.9. Rac1 pull down assay

First, for fusion protein purification, pGEX GST-PBD proteins were prepared from lysates of BL21 *Escherichia coli* induced with 100 μM isopropyl β-d-thiogalactoside (IPTG) for 3 h at 24 °C. Bacteria were lysed in 20 mM HEPES (pH 7.6), 150 mM NaCl, 5 mM $MgCl_2$, 1 mM dithiothreitol DTT, 1 mM PMSF, and 10 μg/ml aprotinin and leupeptin. Recombinant proteins were isolated with glutathione–Sepharose 4B beads (GE Healthcare Life Sciences, Pittsburgh, PA, USA) at 4 °C for 2 h. Beads were sedimented and washed three times in 20 mM HEPES (pH 7.5), 150 mM NaCl, and 1 mM DTT. Then, bound proteins were eluted from the spin column with GST resin using a buffer containing 100 mM Tris-HCL (pH 8), 120 mM NaCl and 20 mM Reduced Glutathione (GSH). Eluted proteins were concentrated using Amicon Ultra-0.5 centrifugal filter units (Sigma-Aldrich).

Rac1–GTP pull-down assays were performed as described previously [31,77]. In brief, cells were allowed to attach to culture plates for 24 h and subsequently lysed in a buffer containing 25 mM HEPES (pH 7.4), 100 mM NaCl, 5 mM $MgCl_2$, 1% NP40, 10% glycerol, 1 mM dithiothreitol and protease inhibitors. Extracts were incubated for 5 min on ice and clarified by centrifugation (10,000*g*, 1 min, 4 °C). Post-nuclear supernatants were used for pull-down assays with 30 μg of GSH beads pre-coated with GST- PBD (to bind Rac1-GTP) per condition. Beads were incubated with extracts for 15 min in a rotating shaker at 4 °C. Thereafter, the beads were collected, washed with lysis buffer containing 0.01% NP40. Bound proteins were solubilized in Laemmli, boiled and then separated by SDS PAGE for Western blotting analysis as indicated above. Numerical values for bands visualized by western blotting were obtained using Image J software (NIH, USA). Results shown were averaged from three independent experiments.

2.10. Trans-endothelial migration assay

TEM assays were performed as described previously [32]. EA.hy926 cells (2.5×10^5were grown to confluency until an endothelial monolayer was formed (after 72 h, as evidenced by Dextran Blue impermeability) on the upper side of 8-μm-pore size membranes (Transwells; BD Biosciences). B16F10 cells (5×10^4) were labeled with CellTracker Green (5 μM; Life Technologies at Thermofisher) and added to the upper chamber of the transwell inserts containing the EA.hy926 monolayer. After 6 h, transwells were washed with PBS and wiped with cotton swabs. Inserts were fixed with 4% paraformaldehyde in PBS, stained with DAPI and mounted onto glass slides. Migrated green labeled-B16F10 cells were imaged by epifluorescence microscopy (IX81, Olympus Latin America Inc., Miami, FL, USA).

2.11. MTS viability assay

B16F10(mock) and B16F10(CAV1) cells (1×10^3 cells/well) were plated on 96- well plates and induced with IPTG for 24 h. After an initial 24-hour period in culture, cells were treated with 10 μM of PP2 or 100 nM of DST for 2 h. Then, cells were washed with 1X PBS and left in complete medium for an additional 2, 4, 24 and 48 h. Cell proliferation was evaluated by the MTS® assay, according to the manufacturer's (Promega, Madison, WI, USA) instructions. As a negative control for cell viability, cells were treated with 1% SDS. Note that the MTS assay evaluates mitochondrial activity and as such provides a measure of cell proliferation and death combined (viability assay).

2.12. Metastasis assays

For metastasis experiments with Src/c-Abl inhibitors, B16F10(mock) or B16F10(CAV1) cells induced with IPTG for 48 h, were previously treated with 10 μM PP2 or 100 nM DST for 2 h and then, suspended in physiological saline solution and injected intravenously into the tail vein of C57BL/6 mice (2×10^5 cells/500 μL

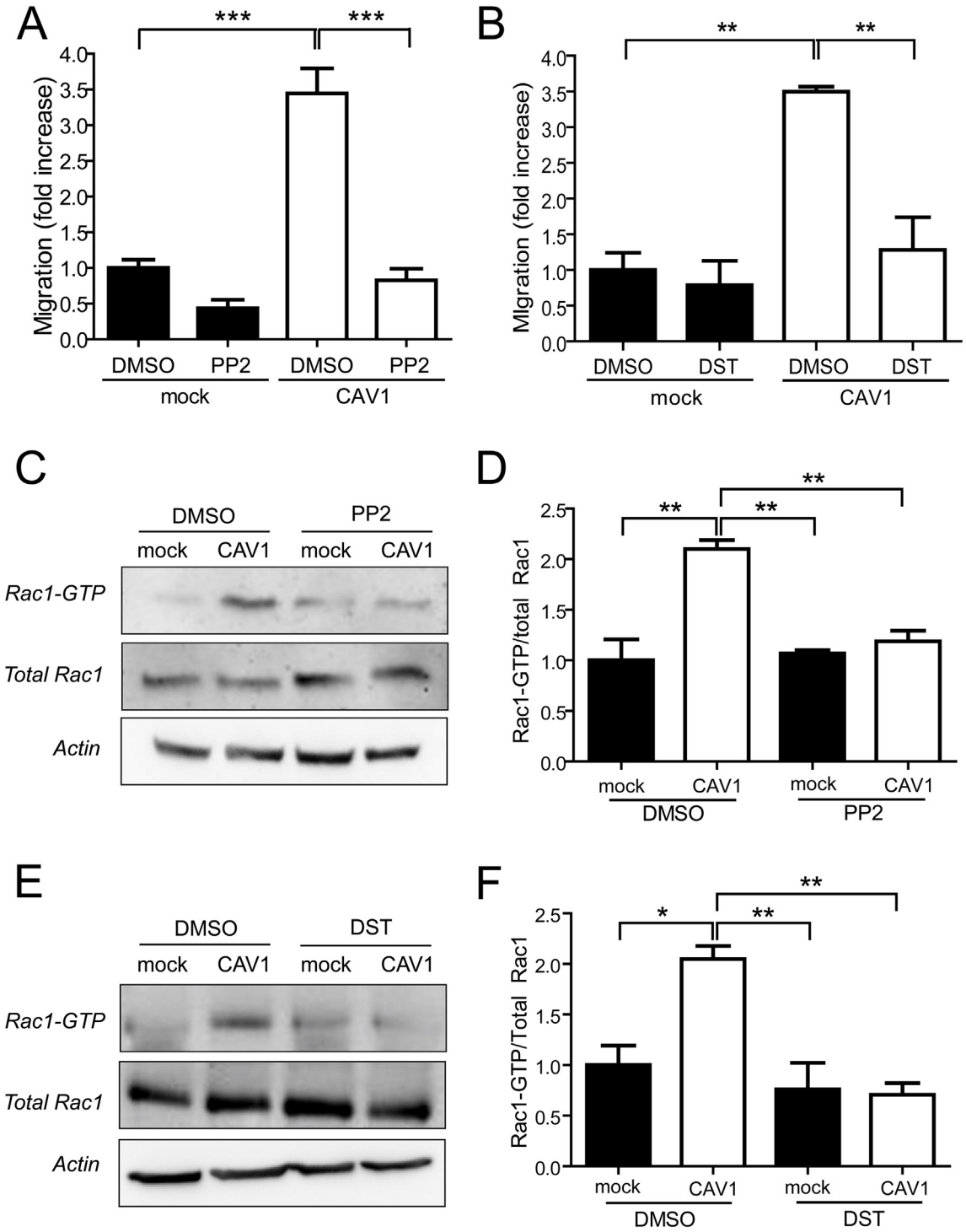

Fig. 1. Caveolin-1-enhanced cell migration and Rac1 activation are blocked by the Src-family kinase inhibitors PP2 and DST. B16F10(mock) and B16F10(CAV1) cells were pre-treated for 2 h with the inhibitors PP2 (10 μM) or DST (100 nM). After washing in PBS, cells (5×10^4) were added to the transwell inserts pre-coated on the lower side with fibronectin (2 μg/ml). Then, cells were allowed to migrate for 2 h and subsequently detected after fixation on the lower side of the membrane by crystal violet staining. **(A)** Migration of cells pre-treated with PP2; **(B)** Migration of cells pre-treated with DST. The graphs show the data averaged from 6 different fields in three independent experiments and normalized to values for B16F10(mock) cells. Rac1–GTP levels were measured with the GST–protein-binding-domain (PBD) pull-down assay. Representative images of western blots selected from three independent experiments showing the levels of active Rac1 in B16F10 cells pre-treated with (**C**) PP2 or **(D)** DST. The numbers below the panels indicate the relative levels of Rac1–GTP, obtained by scanning densitometry analysis and normalization to total Rac1. Data shown represent the average of three independent experiments (mean ± S.E.M, ***p < 0.001; **p < 0.01 and *p < 0.05).

per animal). Animals were euthanized at day 21 post-injection. Lungs were fixed in Fekete's solution [10] and black metastatic nodules were removed to determine tumor mass. Metastasis was expressed as black tissue mass/total lung mass in percent (%) after fixation of the tissue [10,32].

For early *ex vivo* detection of metastasis in mouse lungs, B16F10(mock) and B16F10(CAV1) cells incubated for 24 h in the presence of 1 mM IPTG were exposed for another 24 h to 4 nM of AuNP-

PEG-TAT$_{48-60}$ gold nanoparticles (38). Then, gold nanoparticle labeled cells were treated with 10 μM PP2 or 100 nM DST for 2 h and injected intravenously into the tail vein of C57BL/6 mice (2×10^5 cells/500 μL of saline solution per animal). Animals were maintained for 4 h and then sacrificed. Lungs were fixed in 0.1 M phosphate buffer (pH 7.3)/formaldehyde 10% (v/v) for 48 h at 4 °C. Later, fixed Lungs were dehydrated in alcohol, clarified in Xylene, embedded in paraffin, and sectioned at 5 μm (Leitz 1512 Rotary Microtome, Ontario, Canada). Tissue slices were deparaffinated and hydrated following standard procedures. Antigenicity was recovered treating samples with Retrieval solution (S1699; DACO, Rune Linding, Denmark) at 100 °C for 20 min [57]. Afterwards, tissues were treated with 0.02 M PBS for 5 min, 50 mM Glycine in 0.02 M PBS for 5 min and 0,1% Gelatin-0,05% Tween 20 in 0,02 M PBS for 5 min. Slices were rinsed in water for 10 min and then stained for 15 min in 200 mL of Gold Enhanced™LM (Nanoprobes, NY, USA) per slice. To finalize gold nucleation, sections were rinsed with water according to the landmark protocol [52]. In a final step, slices were counterstained with Hematoxylin (Contrast BLUE Solution) and mounted with Clearmount™ (Invitrogen) [47]. Using identical microscope and camera settings, five digital images per sample were taken to quantify gold nucleation in tissue sections.

This study was performed using male and female C56BL/6 mice housed by the Animal Facility of the Center for studies on Exercise, Metabolism and Cancer (CEMC) according to the rules and standards established by the Bioethics Committee on Animal Research at the Facultad de Medicina, Universidad de Chile (Protocol number CBA # 0416 FMUCH).

2.13. Statistical analysis

Results were statistically compared using the Kruskal-Wallis ANOVA test followed by multiple comparison post-tests (Dunn's multiple comparison test). For paired groups, the Mann-Whitney test was employed. Data analyzed in this manner are specifically indicated in the respective Figure legends. All groups were obtained from three or more independent experiments. *$p < 0.05$ was considered significant.

3. Results

3.1. Caveolin-1-enhanced cell migration is prevented by Src/c-Abl inhibitors in B16F10 melanoma cells

CAV1 phosphorylation on tyrosine-14 by Src family kinases is required to promote migration of non-tumor [37,66,68] and tumor cells [30,31,33,66,73,76]. Our data show that CAV1-enhanced B16F10 melanoma migration and invasion are not enhanced by the non-phosphorylatable Y14F protein, while the phosphomimetic Y14E mutation behaves similar to the wild-type protein [32]. Also, the treatment of B16F10 melanoma and MDA-MB-231 breast cell lines with PP2, a selective pharmacological inhibitor of the Src family kinases, prevents CAV1-enhanced wound closure [31]. Note that the effect is not due to a reduction in total Src levels, because they are comparable in B16F10(mock) and B16F10(CAV1) cells (data not shown). Here we evaluated the effect of pharmacological inhibition of the phosphorylation of CAV1 on tyrosine 14 *in vitro* in migration/invasion assays. To do so, we employed two well-established inhibitors of Src [36,53] and c-Abl [38,74]. To impart clinical relevance to the *in vitro* results, the ability of these inhibitors to prevent CAV1-enhanced metastasis was also tested.

First, we tested the effect of PP2 and DST (selective/reversible inhibitors of Src and c-Abl) on migration of melanoma cells. B16F10 cells were pre-treated with 10 μM PP2 or 100 nM DST for 2 h. As we described previously [31,32], transwell migration increased significantly with the expression of CAV1 in B16F10 cells (2,5 times over control, third bars, Fig. 1A and 1B). Alternatively, pre-treatment of CAV1 expressing cells with PP2 or DST prevented the increase in migration (fourth bars, Fig. 1A and 1B). Note that proliferation was not affected by PP2 or DST in B16F10(mock) and B16F10(CAV1) cells (data not shown). To assess the relevance of tyrosine 14 phosphorylation in downstream signaling events related to migration, we determined the extent of Rac1 activation by pull down assays in B16F10(mock) and B16F10(CAV1) cells pre-treated with the inhibitors. CAV1 expression increased Rac1 activity compared to B16F10(mock) cells, while PP2 prevented this effect (Fig. 1C and 1D). A similar result was obtained with the c-Abl inhibitor, DST (Fig. 1E and F).

These results underscore the relevance of CAV1 tyrosine-14 phosphorylation by Src/c-Abl-kinases in promoting the migration of B16F10 cells *in vitro* through Rac1 activation.

3.2. Caveolin-1-enhanced invasion and gelatinase activity of MMP-2 and MMP-9 are blocked by Src-family kinase inhibitors

Migration of cancer cells through basement membranes and extracellular matrices that contain fibronectin and laminin is an essential step during tumor invasion [69,70,80]. Here, we evaluated the ability of Src/c-Abl-inhibitors to prevent CAV1-enhanced cell invasion using the Matrigel assay. Invasion of B16F10 (CAV1) cells was about 1.5-fold higher than for B16F10(mock) cells (Fig. 2A and 2B), as we previously described [31,32]. Interestingly, pre-incubation of these CAV1 expressing cells with PP2 reduced invasion even below the levels observed for B16F10(mock) cells (Fig. 2A). Also, pre-incubation with DST prevented invasion enhanced by CAV1 in B16F10 cells (Fig. 2B). Expression of MMP-2 and MMP-9 was not affected by treatment of cells with PP2 (Fig. 2C and 2D, respectively); however, the reduction in invasion observed in the presence of PP2 correlated with a statistically significant reduction (*$p < 0.05$) in the gelatinase activity of these proteins (Fig. 2E).

3.3. Caveolin-1-enhanced trans-endothelial migration is blocked by Src-family kinase inhibitors PP2 and DST

Trans-endothelial migration (TEM) is an important step in metastatic colonization of a target tissue. Here, in *in vitro* experiments, CAV1 expression in B16F10 cells augmented migration across an endothelial cell monolayer around 1.5-fold compared with B16F10(mock) cells (Fig. 3A and 3C). Importantly, CAV1-enhanced TEM was prevented by pre-treatment of B16F10 cells with either PP2 or DST (Fig. 3A, 3B and 3C, 3D, respectively).

3.4. c-Abl overexpression in B16F10(CAV1) increases CAV1 protein levels and cell migration

Phosphorylation of CAV1 on tyrosine 14 is implicated in regulation of proteins that promote migration of normal [37,68] and transformed cells [31,32,66,73,76]. Src, Fyn and c-Abl kinases phosphorylate CAV1 in response to several stimuli, including insulin, angiotensin II, osmotic shock, oxidative stress [59,60,78] and also these proteins are associated with focal adhesions [40]. Importantly, CAV1 is a preferred substrate for these tyrosine kinases in cells [49,54,58,67].

Here, we analyzed the expression of c-Abl in B16F10 cells by western blotting (Fig. 4A) and how the kinase modulated the migration of B16F10(mock) and B16F10(CAV1). To that end, cells were transfected with either c-Abl WT or a kinase dead (KD, dominant negative) version of the kinase. Unexpectedly, overexpression of c-Abl WT in B16F10(CAV1) cells significantly increased the levels of total CAV1 as compared to cells transfected with the empty plasmid or a plasmid encoding the dominant negative form of the kinase (Fig. 4B). The increase in pY14-CAV1 levels observed on western blots correlated with the increased levels of total CAV1 in cells transfected with c-Abl WT. As a consequence, the ratio pY14-CAV1/CAV1 did not change compared with the empty plasmid or c-Abl KD conditions (Fig. 4C); however, the total amount of pY14-CAV1 also increased compared to the other

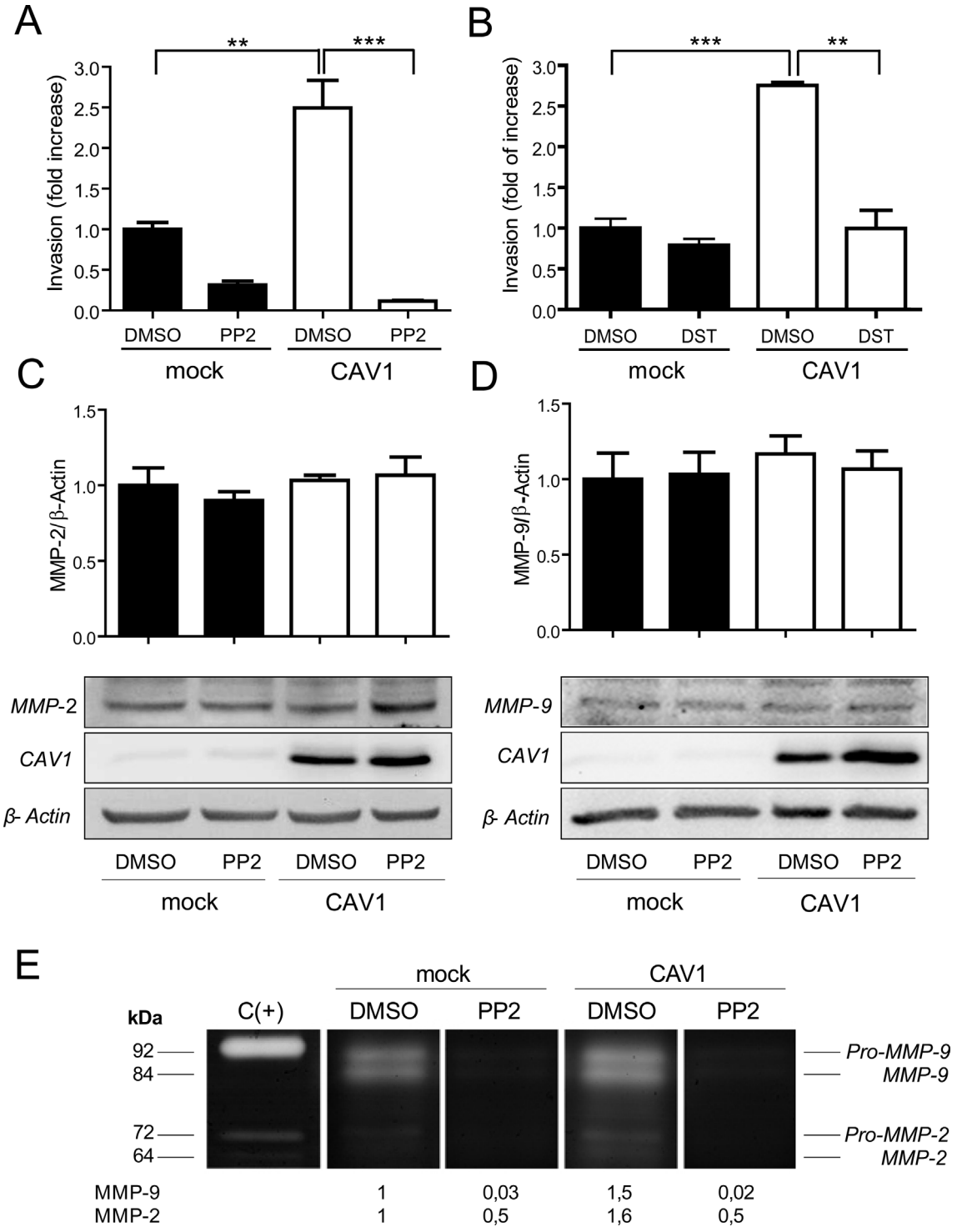

Fig. 2. Caveolin-1-enhanced invasion and gelatinase activity of MMP-2 and MMP-9 are blocked by the Src-family kinase inhibitors. B16F10(mock) and B16F10(CAV1) cells were pre-treated for 2 h with PP2 (10 μM) or DST (100 nM). For invasion assays, cells (5×10^4) were added to matrigel inserts, allowed to invade for 22 h and then detected as described. **(A)** Invasion of cells pre-treated with PP2; **(B)** Invasion of cells pre-treated with DST. The graphs show the data averaged from 6 different fields in three independent experiments and normalized to values for B16F10(mock) cells (mean ± S.E.M, ***$p < 0.001$ and **$p < 0.01$). B16F10(mock) and B16F10(CAV1) cells induced with IPTG for 48 h were serum-starved for 16 h and then treated with PP2 for 2 h. Total protein extracts were obtained for analysis of metalloproteinase expression in cells. Representative images of western blots selected from three independent experiments showing levels of total MMP-2 **(C)** and total MMP-9 **(D)**. The relative expression of proteins was evaluated by scanning densitometry using Image J software. The graphs show the values of the densitometric analysis, normalized to the B16F10(mock) (DMSO) control. Supernatants were collected and analyzed by zymography to determine the enzymatic activity of MMP-2 and MMP-9. **(E)** Degradation of gelatin due to the gelatinase activity of MMPs was evaluated by densitometric analysis of the clear bands in the gels using the Image J software (NIH, USA). The image is representative of results obtained in three independent experiments. Numbers below each lane indicate the relative activity for MMP-2 and MMP-9, normalized to the loading control (see Materials and Methods). Values were normalized with respect to the control condition [B16F10(mock)/DMSO]. Data shown are the averages of three independent experiments.

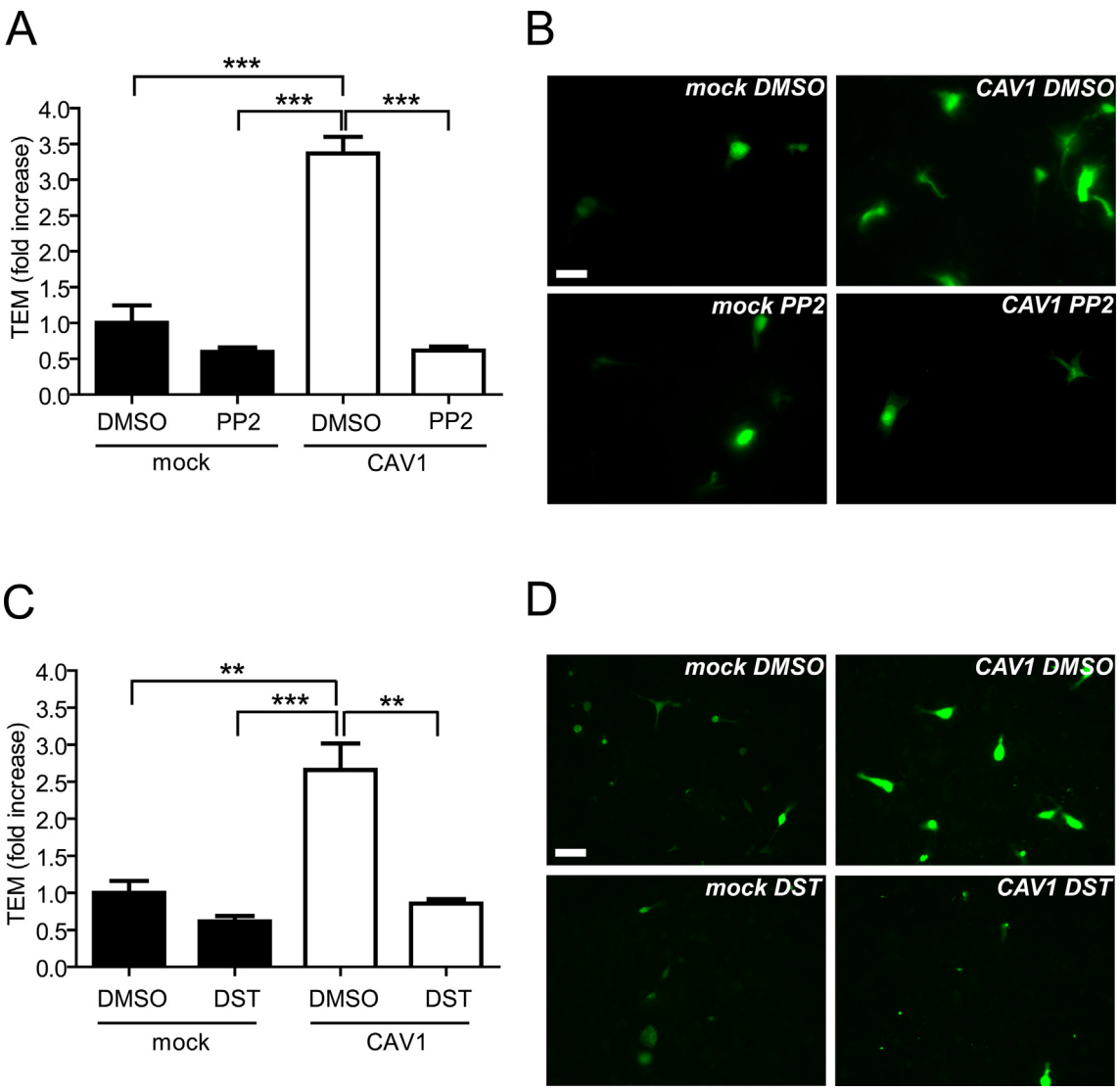

Fig. 3. Caveolin-1-enhanced trans-endothelial migration is blocked by the Src-family kinase inhibitors PP2 and DST. EA.hy926 cells ($2{,}5 \times 10^5$) were seeded on the Transwell inserts and impermeable cell monolayers were allowed to form for 72 h. B16F10(mock) and B16F10(CAV1) cells (5×10^4), previously stained with CellTracker Green and pre-treated with PP2 or DST for 2 h, were added to the confluent EA.hy926 monolayer. Then, B16F10 cells were allowed to penetrate the EA.hy926 monolayer for 6 h. Cells were observed and quantified by epifluorescence microscopy with a 40X objective on the lower side of the Transwell membranes (scale bar, 50 μm). Values in the graphs represent the average values for TEM (cells per field) following incubation of the B16F10 cells with **(A)** PP2 or **(C)** DST. Data were normalized to values obtained for control B16F10(mock) cells. Images of B16F10(mock) and B16F10(CAV1) cells pre-treated with **(B)** PP2 or (**D**) DST. TEM was quantified as cells per field from 10 different fields in three independent experiments (mean ± S.E.M, ***$p < 0.001$ and **$p < 0.01$). (For interpretation of the references to colour in this figure legend, the reader is referred to the web version of this article.)

conditions (Fig. 4D). Moreover, in cells transfected with c-Abl WT, migration increased even in B16F10(mock) cells but the increase was substantially greater in CAV1 expressing cells (Fig. 4E; third and fourth bars). On the other hand, migration of B16F10(CAV1) cells was significantly reduced by the transfection with the c-Abl KD plasmid (Fig. 4E, fifth and sixth bars).

3.5. Caveolin-1-enhanced lung metastasis in C57BL/6 mice is reduced by PP2 or DST

We have previously reported on the importance of tyrosine 14 for CAV1-enhanced migration, invasion and metastasis [31,32]. To determine the relevance of phosphorylation at this site for CAV1 function in metastasis, we injected mice with B16F10(mock) and B16F10(CAV1) previously treated with PP2 or DST. As expected, expression of CAV1 significantly increased lung metastasis of B16F10 cells injected intravenously into syngeneic C57BL/6 mice, as compared to B16F10(mock) cells. However, when B16F10(CAV1) cells were previously treated with PP2, lung metastasis was prevented (Fig. 5A). Likewise, metastasis was prevented by pre-treatment of cells with DST (Fig. 5B).

To determine the extent to which phosphorylation of CAV1 might be relevant to the initial steps of metastasis, B16F10 cells were pre-treated with PP2 or DST for 2 h, then the culture medium was changed and pY14-CAV1 levels were evaluated at different time points. Levels of pY14-CAV1 in cells pre-treated with PP2 or DST were significantly reduced compared with control (DMSO) after 2 h (Fig. 5C and 5D, respectively). Then, phosphorylation of CAV1 on tyrosine 14 increased up to the initial levels 12 h after eliminating the inhibitors (Fig. 5C and 5D). These results show that, even after removal of either inhibitor, pY14 levels were maintained low for at least 2–4 h in B16F10 cells and this was sufficient to reduce significantly lung metastasis in mice after 21 days (Fig. 5A and 5B), suggesting that Y14 phosphorylation of CAV1 was relevant for very early steps of metastasis.

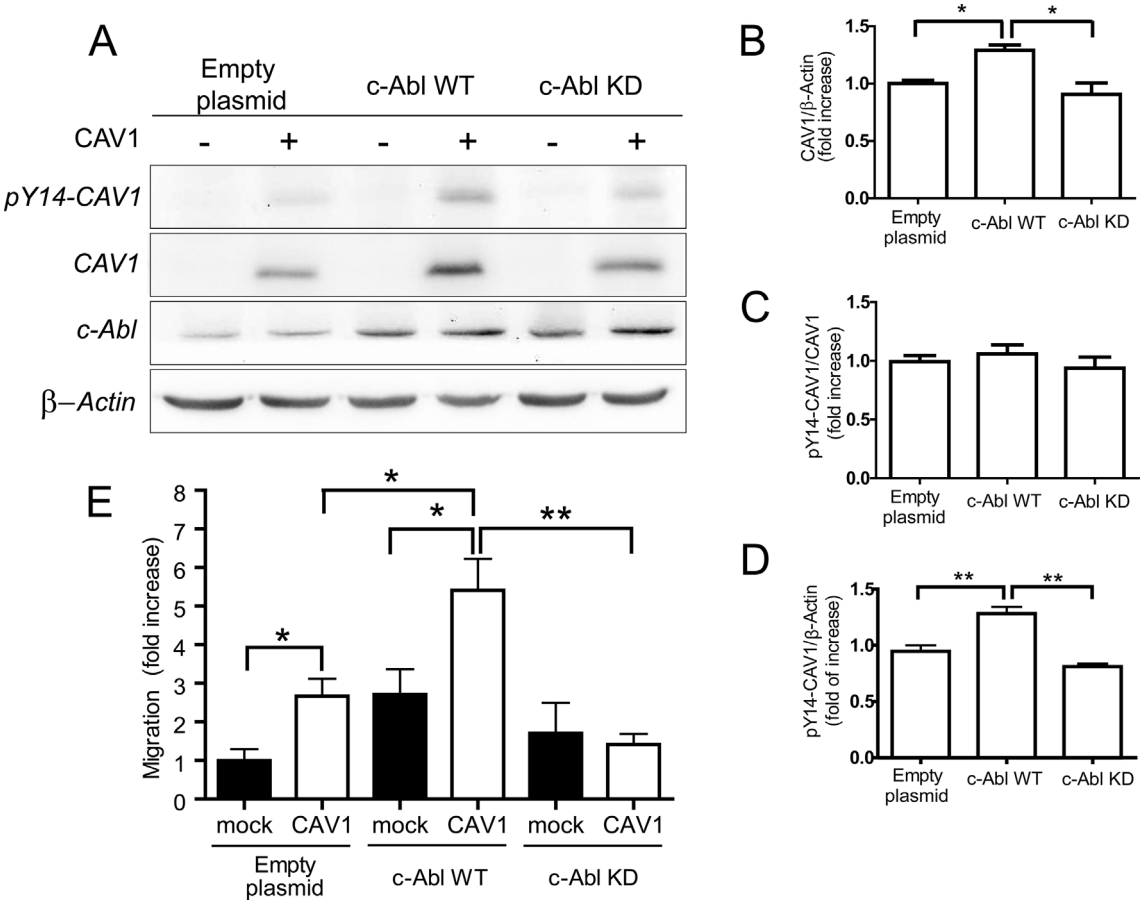

Fig. 4. c-Abl overexpression in B16F10(CAV1) increases CAV1 protein levels and cell migration. B16F10(mock) and B16F10(CAV1) cells were transfected with c-Abl-GFP, c-Abl– KD-GFP (kinase death dominant-negative form of c-Abl) or the GFP empty plasmids and then induced by IPTG for 48 h. Protein extracts were analyzed by western blotting for c-Abl, CAV1 and pY14-CAV1 levels. (A) Western blot representative of results obtained in three independent experiments shows total levels of pY14-CAV1, CAV1 and c-Abl. β-Actin is included as a loading control. The relative expression of proteins was evaluated by scanning densitometry using Image J software. Values in the graphs show the levels of total CAV1 relative to β-Actin (B), of pY14-CAV1 relative to total CAV1 (C), and of pY14-CAV1 relative to β-Actin (D). Data in the graphs were normalized to the respective mock/empty vector (control) value. (E) Migration of B16F10(mock) and B16F10(CAV1) cells transfected with c-Abl-GFP, c-Abl–KD-GFP or the GFP empty plasmids. The graph shows the data averaged from 6 different fields in three independent experiments and normalized to values for B16F10(mock) cells. Data shown represent the average of three independent experiments (mean ± S.E.M, $^{**}p < 0.01$ and $^{*}p < 0.05$).

3.6. Caveolin-1-enhanced lung metastasis detected after 4 h is prevented by pre-treatment of B16F10 cells with Src-family kinase inhibitors

To corroborate that Y14 phosphorylation was essential during early steps of metastasis, B16F10(mock) and B16F10(CAV1) cells were labeled with AuNP-PEG-TAT$_{48\text{-}60}$ gold nanoparticles (38), pre-treated with PP2, DST or vehicle (DMSO) and then injected into the tail vein of mice. Animals were maintained for 4 h and then sacrificed. Lungs were fixed and stained with Gold Enhanced™LM to detect gold nucleation. The results of Fig. 6 show positive gold (Au) nuclei detected in lung parenchyma after 4 h (see digital zoom of the gold (Au) positive cells). As anticipated, CAV1 expression in B16F10 cells significantly increased the number of gold (Au) positive nuclei in lungs 4 h post injection compared to B16F10(mock) cells (Fig. 6A, red arrows; Fig. 6B). However, when B16F10(CAV1) cells were pre-treated with PP2, gold (Au) positive nuclei did not increase significantly. A similar effect was observed with DST, albeit to a lesser extent (Fig. 6C).

4. Discussion

Caveolin-1 expression is reduced in the early stages of cell transformation and tumor development, consistent with a role as a tumor suppressor. At later stages of cancer progression, re-expression of the protein is associated with enhanced malignancy (multidrug resistance and metastasis). Interestingly, studies from our group have shown in a preclinical experimental model that expression of the protein in melanoma cells reduces subcutaneous tumor growth while promoting metastasis to the lung following surgical removal of an existing tumor. Thus, elevated CAV1 expression need not necessarily be bad [10]. However, phosphorylation of CAV1 on tyrosine-14 promotes tumor cell migration, invasion and metastasis [46]. CAV1(Y14) is a substrate for the tyrosine kinases Src and c-Abl [56], and induces migration by modulating Rac1 activity in cancer cells [31,44]. Thus, potentially beneficial effects associated with elevated CAV1 expression may be preserved as long as phosphorylation is prevented. Here we evaluated the ability of two tyrosine kinase inhibitors (PP2 and DST) to block the metastatic potential of melanoma cells. The findings show that exposure of B16F10 cells to these tyrosine kinase inhibitors reduces Rac1 activation, migration, MMP activity, invasion and TEM *in vitro*, as well as metastasis *in vivo* by reducing CAV1 phosphorylation.

Src and c-Abl are cytoplasmatic tyrosine kinases implicated in many cellular processes and cancer development. Because of their similarity, several compounds originally synthesized as Src inhibitors are also c-Abl inhibitors. Consistent with this, DST and PP2 are reportedly dual Src and c-Abl inhibitors [64]. DST is an ATP-binding inhibitor of c-Abl and Src-family kinases, as well as c-KIT, PDGFR-alpha and beta, and ephrin receptor kinase, and has been approved by the United States Food and Drug Administration (FDA) for the treatment of leukemia.

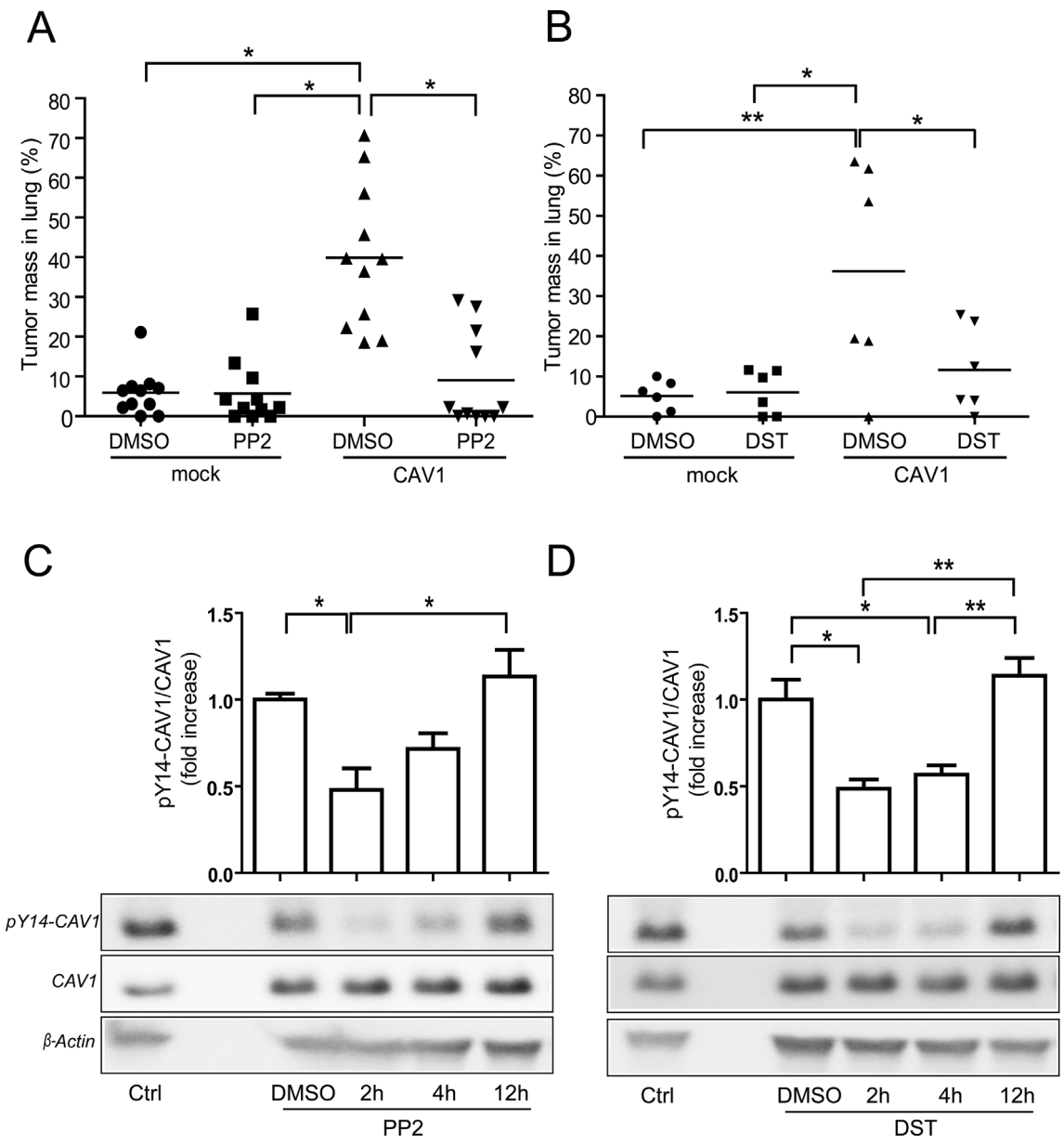

Fig. 5. Caveolin-1-enhanced lung metastasis in C57BL/6 mice is prevented by the Src-family kinase inhibitors PP2 and DST. C57BL/6 mice were intravenously injected with B16F10(mock) or B16F10(CAV1) cells (5×10^5) previously grown for 48 h in the presence of IPTG (1 mM) and then pre-treated for 2 h with either 10 μM PP2 or 100 nM DST. (A) Graph summarizing the values observed for the metastatic lung mass of animals at day 21 after the inoculation with B16F10 cells pre-incubated with either DMSO or PP2 (44 mice in total, 11 per group). (B) Graph summarizing the values observed for the metastatic lung mass of animals at day 21 after the inoculation with B16F10 cells pre-incubated with either DMSO or DST (24 mice in total, 6 per group). Statistically significant differences are indicated (**$p < 0.01$ and *$p < 0.05$). Levels of pY14-CAV1 in three different experiments before pre-treatment with the inhibitors were analyzed. B16F10(CAV1) cells were incubated with PP2, DST or vehicle (DMSO), washed and total protein extracts were obtained for western blot analysis. A control (Ctrl) without inhibitor or vehicle was also included. (C) Total levels of pY14-CAV1 at 2, 4 and 12 h after PP2 removal. (D) Total levels of pY14-CAV1 at 2, 4 and 12 h after DST pre-incubation. The graphs show the densitometric analysis of pY14-CAV1 normalized to total CAV1. Images are representative of three independent experiments (mean ± S.E.M, **$p < 0.01$ and *$p < 0.05$).

However, the potential utility of DST in treating solid tumors remains to be established. While some studies did not observe beneficial effects of DST in the treatment of solid tumors, others found evidence indicating that this inhibitor may be useful. For instance, the clinical activity of DST in pancreatic refractory tumors is modest [63] and did not significantly prolong survival in clinical trials with prostate cancer patients [45].

On the other hand, DST displayed anti-tumor activity with a subset of colorectal cancer cells in a mouse explant model. In doing so, Src inhibition has become an attractive target for treatment of colorectal cancer [75]. In addition, lung cancers overexpressing Yes, a Src-family kinase, are highly sensitive to DST in patient-derived xenograft models [48]. Moreover, bosutinib, a Src/c-Abl inhibitor, is effective in human pancreatic cancer-derived xenograft models expressing high levels of CAV1 [62]. These observations provide support for the clinical evaluation of DST treatment in selected subsets of patients with altered Src family kinase and/or CAV1 status as predictive biomarkers for therapy.

CAV1 has been implicated in oncogenic cell transformation, tumor progression, resistance to therapy and metastasis [5–8,43]. In particular, CAV1 activates a Rab5/Rac1 signaling pathway and thereby enhances tumor cell migration and invasion [44]. In addition, other authors have reported that Y14-CAV1 phosphorylation promotes focal

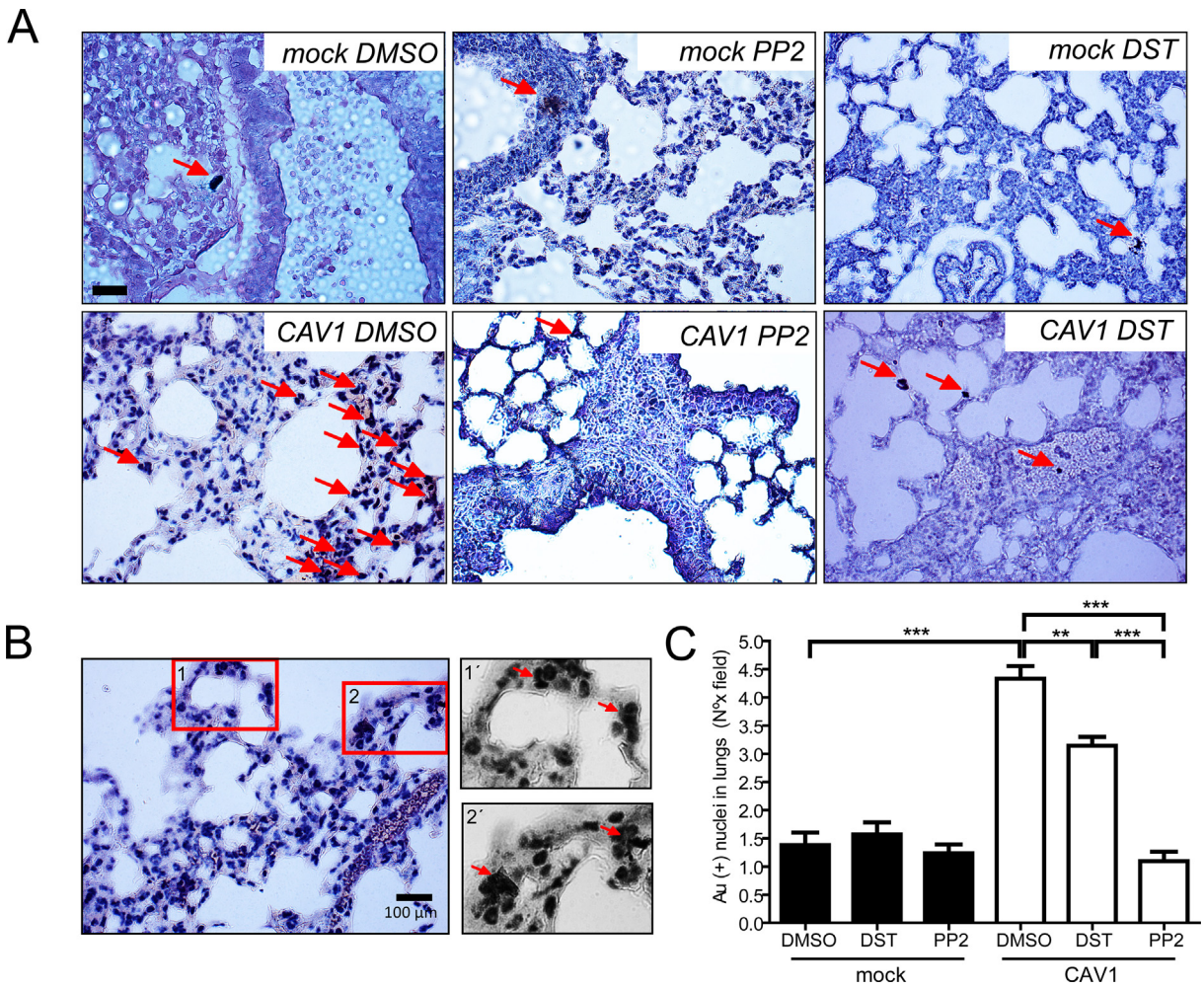

Fig. 6. Caveolin-1 enhanced metastasis, detected in lungs of recipient mice as early as 4 h after intravenous injection of cells, is prevented by pre-treatment with Src-family kinase inhibitors. B16F10(mock) and B16F10(CAV1) cells (2×10^5) labeled with AuNP-PEG-TAT48-60, were pre-treated with PP2, DST or vehicle (DMSO) and resuspended in 500 µL of physiological saline for injection into the tail vein of mice. Animals were maintained for 4 h and then sacrificed. Lungs were fixed and stained with Gold Enhanced™LM to detect gold nucleation. Slices were counterstained with hematoxylin and mounted. Using identical microscope and camera settings, five digital images per condition were taken to quantify gold nucleation in tissue sections. (A) Images are representative of four animals per group. Gold nuclei are indicated with red arrows. Scale bar of 100 µm. (B) Images of gold Au(+) nuclei in lungs of recipient mice intravenously injected with B16F10(CAV1) cells. Gold (Au) nuclei are highlighted in red rectangles (1 and 2). Magnification bar 100 µm. 1́ and 2́ show digital zooms of the aforementioned gold nuclei that correspond to metastatic mass in the lung parenchyma. (C) The graph shows the number of gold (Au) positive nuclei in histological sections of the mouse lungs. Data are representative of three independent experiments (mean ± S.E.M, ***$p < 0.001$ and **$p < 0.01$). (For interpretation of the references to colour in this figure legend, the reader is referred to the web version of this article.)

adhesion turnover and, thereby, cancer cell motility [32,33,56,61]. This phosphorylation is mediated by Src family tyrosine kinases, including c-Abl [28,40]. Consistent with these reports, we observed here that the overexpression of c-Abl increases CAV1 phosphorylated on tyrosine-14 and, as a consequence, cell migration. However, somewhat surprisingly, the increase in Y14 phosphorylation was paralleled by an increase in CAV1 protein levels. The mechanistical underpinnings responsible for this increase in protein expression remain to be determined, but as a consequence there was more phospho Y14-CAV1 in c-Abl expressing B16F10 cells. In addition, Y14-CAV1 phosphorylation is prevented transiently by the pre-incubation with PP2 and DST for 2 h, which consequently reduced active Rac1 levels and cell migration, as well as MMP2/9 activity, invasion, and TEM. In vivo, these effects translate into a reduction in early attachment of B16F10 cells to the lung parenchyma, as well as significant inhibition of the colonization and the development of metastases in this tissue (Fig. 7).

As our group previously demonstrated, B16F10 cells can be detected in mouse lungs as early as 5 min after intravenous injection into the tail vein [42]. On the other hand, our *in vitro* experiments have shown that fibronectin and laminin, two abundant components of ECM in lung stimulate phosphorylation of CAV1 on tyrosine 14 [32]. Of note, both inhibitors (PP2 and DST) are reversible and phosphorylation of CAV1 on tyrosine-14 in cells starts recovering 2–4 h after inhibitor removal. Despite this being the case, pre-incubation of cells with either inhibitor sufficed to reduce CAV1-enhanced metastasis, suggesting that Y14-CAV1 phosphorylation is required during the first steps of the metastatic process.

Data from the literature in cancer models show a positive correlation between CAV1 expression and the activity of MMP-2 and MMP-9 [72]. In human breast cancer cell lines, lipid rafts and CAV1 are required for invadopodia formation. There, the transmembrane metalloprotease MT1-MMP, the main activator of MMP-2 [71] co-localizes with CAV1, which is important for further ECM degradation during invasion [79]. Others have shown in non-tumor cells that phosphorylation of CAV1 on Y14 mediated by Src is necessary for its interaction with MT1-MMP in caveolae [55], suggesting an important role for CAV1 phosphorylation during cell invasion by promoting ECM degradation [41]. Our results show that Src/Abl inhibitors significantly

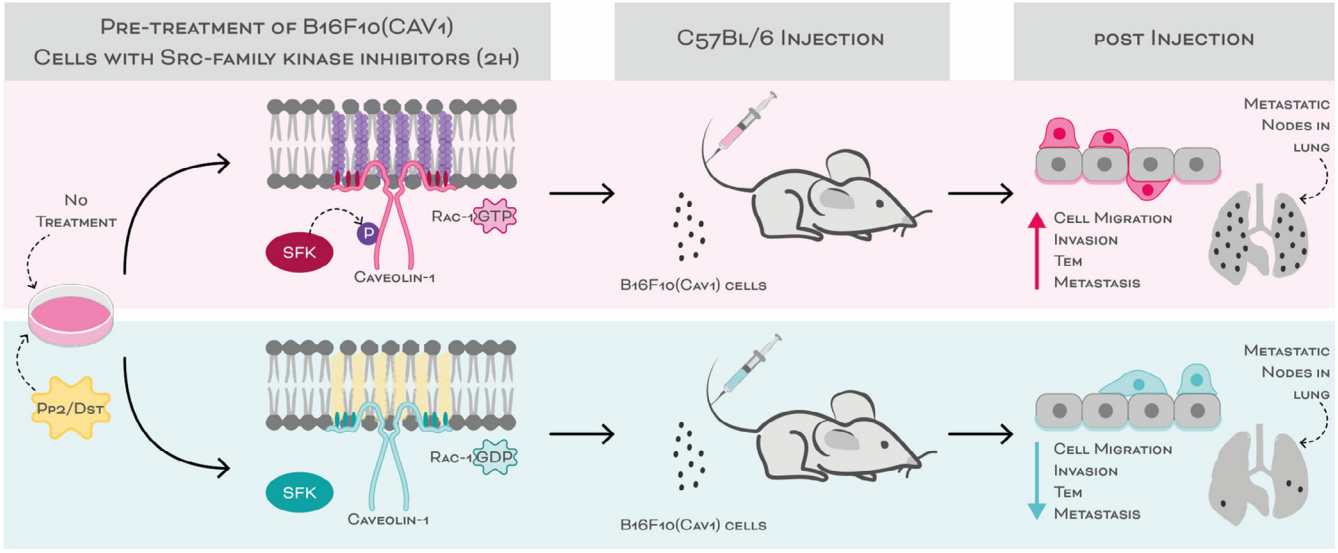

Fig. 7. Phosphorylation of CAV1 on tyrosine-14 as an important early step during lung colonization by melanoma in C57BL/6 mice. Pretreatment for 2 h of B16F10(CAV1) cells with PP2 or DST inhibits transiently the phosphorylation on tyrosine-14, which prevents activation of Rac1, migration, invasion and TEM *in vitro*. *In vivo* this reduces adhesion and lung colonization by melanoma cells (rapid effects within hours), as well as the formation of metastatic lung nodules after 21 days.

reduce MMP-2 and MMP-9 activity, which, based on the aforementioned data available in the literature, is likely attributable to the decrease in pY14-CAV1.

In a previous study, we established a protocol that permits labeling of the B16F10 with gold nanoparticles prior to injection into mice and then following how the cells colonize the lung at different time intervals, as determined *ex-vivo* by fluorescence and optical microscopy using gold enhancement technology [51]. According to those studies, CAV1 presence promotes very early steps of lung colonization. However, whether CAV1 phosphorylation is relevant in this context was not clear. Our studies here identify CAV1 phosphorylation as the driving force for enhanced lung colonization due to the presence of the protein during the first 2–4 h. This insight provides a window of therapeutic opportunity for those patients where enhanced CAV1 expression is associated with poor prognosis. In those cases, surgical procedures to remove solid tumors could be complemented with local treatments using these inhibitors to prevent post-surgery metastasis.

In conclusion, our study reveals that CAV1 phosphorylation by Src-family kinases is crucial to the initial steps of lung metastasis in a preclinical animal model. In doing so, we provide evidence that supports the use of these Src-family kinase inhibitors in clinical trials as therapeutics to prevent metastasis of solid tumors expressing high CAV1 levels.

CRediT authorship contribution statement

Rina Ortiz: Investigation, Methodology, Formal analysis, Validation, Funding acquisition, Data curation, Visualization, Writing - original draft, Writing - review & editing. **Jorge Díaz:** Investigation, Formal analysis, Validation. **Natalia Díaz-Valdivia:** Investigation, Formal analysis, Validation. **Samuel Martínez:** Investigation, Formal analysis. **Layla Simón:** Investigation. **Pamela Contreras:** Investigation. **Lorena Lobos-González:** Investigation. **Simón Guerrero:** Investigation. **Lisette Leyton:** Conceptualization, Methodology, Funding acquisition, Data curation, Writing - review & editing, Visualization, Supervision, Resources. **Andrew F.G. Quest:** Conceptualization, Methodology, Formal analysis, Validation, Funding acquisition, Project administration, Writing - review & editing, Visualization, Supervision, Resources.

Acknowledgements

Dr. Alejandra Alvarez is greatly acknowledged for providing the c-Abl encoding plasmids. Bonhomía Ltda. (@bonhomia.grafica), Santiago, Chile is acknowledged for designing the summary (Fig. 7) and the graphical abstract.

Grant support

This work was supported by CONICYT PAI CONVOCATORIA NACIONAL SUBVENCIÓN A INSTALACIÓN EN LA ACADEMIA CONVOCATORIA AÑO 2018 PAI77180019 (RO). CONICYT-FONDAP 15130011 (AFGQ), FONDECYT 1130250, 1170925 (AFGQ), Anillo ACT 1111 (AFGQ), FONDECYT 1150744, 1200836 (LL), FONDECYT 1140907 (VAT), and CONICYT PhD fellowships (NDV, JD, AC), FONDECYT 11140204 (LLG), BASAL CCTE-PFB16 CONICYT (LLG).

Conflicts of interest

The authors declare no conflicts of interest.

References

[1] H.N. Fridolfsson, et al., Regulation of intracellular signaling and function by caveolin, FASEB J. 28 (9) (2014) 3823–3831, https://doi.org/10.1096/fj.14-252320.
[2] M.A. Fernandez-Rojo, G.A. Ramm, Caveolin-1 function in liver physiology and disease, Trends Mol. Med. 22 (10) (2016) 889–904, https://doi.org/10.1016/j.molmed.2016.08.007.
[3] A. Mergia, The role of caveolin 1 in HIV infection and pathogenesis, Viruses 9 (129) (2017) 1–26, https://doi.org/10.3390/v9060129.
[4] R. Kulshrestha, et al., Caveolin-1 as a critical component in the pathogenesis of lung fibrosis of different etiology: Evidences and mechanisms, Exp. Mol. Pathol. 111 (2019) 104315, , https://doi.org/10.1016/j.yexmp.2019.104315.
[5] A.J. Koleske, D. Baltimore, M.P. Lisanti, Reduction of caveolin and caveolae in oncogenically transformed cells, PNAS 92 (5) (1995) 1381–1385, https://doi.org/10.1073/pnas.92.5.1381.
[6] F.C. Bender, et al., Caveolin-1 levels are down-regulated in human colon tumors, and ectopic expression of caveolin-1 in colon carcinoma cell lines reduces cell tumorigenicity, Cancer Res. 60 (20) (2000) 5870–5878.
[7] T.M. Williams, M.P. Lisanti, Caveolin-1 in oncogenic transformation, cancer, and metastasis, Am. J. Physiol.-Cell Physiol. 288 (3) (2005) C494–C506, https://doi.org/10.1152/ajpcell.00458.2004.
[8] A.F.G. Quest, J.L. Gutierrez-Pajares, V.A. Torres, Caveolin-1: An ambiguous partner in cell signalling and cancer, J. Cell Mol. Med. 12 (4) (2008) 1130–1150, https://doi.org/10.1111/j.1582-4934.2008.00331.x.
[9] F. Felicetti, et al., Caveolin-1 tumor-promoting role in human melanoma, Int. J.

Cancer 125 (7) (2009) 1514–1522, https://doi.org/10.1002/ijc.24451.
[10] L. Lobos-González, et al., E-cadherin determines Caveolin-1 tumor suppression or metastasis enhancing function in melanoma cells, Pigment Cell and Melanoma Research 26 (4) (2013) 555–570, https://doi.org/10.1111/pcmr.12085.
[11] J.J. Bravo-Cordero, L. Hodgson, J. Condeelis, Directed cell invasion and migration during metastasis, Curr. Opin. Cell Biol. 24 (2) (2012) 277–283, https://doi.org/10.1016/j.ceb.2011.12.004.
[12] F. Spill, et al., Impact of the physical microenvironment on tumor progression and metastasis, Curr. Opin. Biotechnol. 40 (2016) 41–48, https://doi.org/10.1016/j.copbio.2016.02.007.
[13] J.M. Drake, et al., ZEB1 enhances transendothelial migration and represses the epithelial phenotype of prostate cancer cells, Mol. Biol. Cell 20 (8) (2009) 2207–2217, https://doi.org/10.1091/mbc.E08-10-1076.
[14] F.L. Miles, et al., Stepping out of the flow: Capillary extravasation in cancer metastasis, Clin. Exp. Metastasis 25 (2008) 305–324, https://doi.org/10.1007/s10585-007-9098-2.
[15] A. Navarro, B. Anand-Apte, M.O. Parat, A role for caveolae in cell migration, FASEB J. 18 (15) (2004) 1801–1811, https://doi.org/10.1096/fj.04-2516rev.
[16] T.C. Thompson, Metastasis-related genes in prostate cancer: The role of caveolin-1, Cancer Metastasis Rev. 17 (4) (1998) 439–442, https://doi.org/10.1023/A:1006110326366.
[17] G. Yang, et al., Elevated expression of caveolin is associated with prostate and breast cancer, Clin. Cancer Res. 4 (8) (1998) 1873–1880.
[18] K. Bełkot, M. Bubka, A. Lityńska, Expression of caveolin-1 in human cutaneous and uveal melanoma cells, Folia Biologica (Poland) 64 (3) (2016) 145–151, https://doi.org/10.3409/fb64_3.145.
[19] L. Campbell, M. Gumbleton, D.F.R. Griffiths, Caveolin-1 overexpression predicts poor disease-free survival of patients with clinically confined renal cell carcinoma, Br. J. Cancer 89 (10) (2003) 1909–1913, https://doi.org/10.1038/sj.bjc.6601359.
[20] T. Ando, et al., The overexpression of caveolin-1 and caveolin-2 correlates with a poor prognosis and tumor progression in esophageal squamous cell carcinoma, Oncol. Rep. 18 (3) (2007) 601–609, https://doi.org/10.3892/or.18.3.601.
[21] L. Campbell, et al., Combined expression of caveolin-1 and an activated AKT/mTOR pathway predicts reduced disease-free survival in clinically confined renal cell carcinoma, Br. J. Cancer 98 (5) (2008) 931–940, https://doi.org/10.1038/sj.bjc.6604243.
[22] Y. Tang, et al., Caveolin-1 is related to invasion, survival, and poor prognosis in hepatocellular cancer, Med. Oncol. 29 (2) (2012) 977–984, https://doi.org/10.1007/s12032-011-9900-5.
[23] T. Okamoto, et al., Caveolins, a family of scaffolding proteins for organizing "pre-assembled signaling complexes" at the plasma membrane, J. Biol. Chem. 273 (10) (1998) 5419–5422, https://doi.org/10.1074/jbc.273.10.5419.
[24] H. Kogo, T. Aiba, T. Fujimoto, Cell type-specific occurrence of caveolin-1α and -1β in the lung caused by expression of distinct mRNAs, J. Biol. Chem. 279 (24) (2004) 25574–25581, https://doi.org/10.1074/jbc.M310807200.
[25] A. Nohe, et al., Dynamics and interaction of caveolin-1 isoforms with BMP-receptors, J. Cell Sci. 118 (3) (2005) 643–650, https://doi.org/10.1242/jcs.01402.
[26] P.K. Fang, et al., Caveolin-1α and -1β perform nonredundant roles in early vertebrate development, Am. J. Pathol. 169 (6) (2006) 2209–2222, https://doi.org/10.2353/ajpath.2006.060562.
[27] S. Li, R. Seitz, M.P. Lisanti, Phosphorylation of caveolin by Src tyrosine kinases: The α-isoform of caveolin is selectively phosphorylated by v-Src in vivo, J. Biol. Chem. 271 (7) (1996) 3863–3868, https://doi.org/10.1074/jbc.271.7.3863.
[28] A.R. Sanguinetti, C.C. Mastick, C-Abl is required for oxidative stress-induced phosphorylation of caveolin-1 on tyrosine 14, Cell. Signal. 15 (3) (2003) 289–298, https://doi.org/10.1016/S0898-6568(02)00090-6.
[29] A.R. Sanguinetti, H. Cao, C. Corley Mastick, Fyn is required for oxidative- and hyperosmotic-stress-induced tyrosine phosphorylation of caveolin-1, Biochem. J 376 (1) (2003) 159–168, https://doi.org/10.1042/BJ20030336.
[30] J.G. Goetz, et al., Concerted regulation of focal adhesion dynamics by galectin-3 and tyrosine-phosphorylated caveolin-1, J. Cell Biol. 180 (6) (2008) 1261–1275, https://doi.org/10.1083/jcb.200709019.
[31] H. Urra, et al., Caveolin-1-enhanced motility and focal adhesion turnover require tyrosine-14 but not accumulation to the rear in metastatic cancer cells, PLoS ONE 7 (4) (2012) e33085, , https://doi.org/10.1371/journal.pone.0033085.
[32] R. Ortiz, et al., Extracellular matrix-specific Caveolin-1 phosphorylation on tyrosine 14 is linked to augmented melanoma metastasis but not tumorigenesis, Oncotarget 7 (26) (2016) 40571–40593, https://doi.org/10.18632/oncotarget.9738.
[33] B. Joshi, et al., Phosphorylated caveolin-1 regulates Rho/ROCK-dependent focal adhesion dynamics and tumor cell migration and invasion, Cancer Res. 68 (20) (2008) 8210–8220, https://doi.org/10.1158/0008-5472.CAN-08-0343.
[34] N.I. Díaz-Valdivia et al. 'The non-receptor tyrosine phosphatase type 14 blocks caveolin-1-enhanced cancer cell metastasis', Oncogene 2020 Springer US 10.1038/s41388-020-1242-3.
[35] J. Araujo, C. Logothetis, Dasatinib: a potent SRC inhibitor in clinical development for the treatment of solid tumors, Cancer Treat. Rev. 36 (2010) 492–500, https://doi.org/10.1016/j.ctrv.2010.02.015.
[36] J. Bain, et al., The specificities of protein kinase inhibitors: an update, Biochem. J 371 (1) (2003) 199–204, https://doi.org/10.1042/BJ20021535.
[37] A. Beardsley, et al., Loss of caveolin-1 polarity impedes endothelial cell polarization and directional movement, J. Biol. Chem. 280 (5) (2005) 3541–3547, https://doi.org/10.1074/jbc.M409040200.
[38] S. Blake, et al., The Src/ABL kinase inhibitor dasatinib (BMS-354825) inhibits function of normal human T-lymphocytes in vitro, Clin. Immunol. 127 (3) (2008) 330–339, https://doi.org/10.1016/j.clim.2008.02.006.
[39] R. Buettner, et al., Inhibition of Src family kinases with dasatinib blocks migration and invasion of human melanoma cells, Mol. Cancer Res. 6 (11) (2008) 1766–1774, https://doi.org/10.1158/1541-7786.MCR-08-0169.
[40] H. Cao, W.E. Courchesne, C.C. Mastick, A phosphotyrosine-dependent protein interaction screen reveals a role for phosphorylation of caveolin-1 on tyrosine 14. Recruitment of C-terminal Src kinase, J. Biol. Chem. 277 (11) (2002) 8771–8774, https://doi.org/10.1074/jbc.C100661200.
[41] M. Cokakli, et al., Differential expression of Caveolin-1 in hepatocellular carcinoma: Correlation with differentiation state, motility and invasion, BMC Cancer 9 (65) (2009), https://doi.org/10.1186/1471-2407-9-65.
[42] V.M. Díaz-García, et al., (2018) 'Biomimetic quantum dot-labeled B16F10 murine melanoma cells as a tool to monitor early steps of lung metastasis by in vivo imaging', Int. J. Nanomed. 13 (2018) 6391–6412, https://doi.org/10.2147/IJN.S165565.
[43] N.I. Díaz-Valdivia, et al., Anti-neoplastic drugs increase caveolin-1-dependent migration, invasion and metastasis of cancer cells, Oncotarget 8 (67) (2017) 111943–111965, https://doi.org/10.18632/oncotarget.22955.
[44] J. Díaz, et al., Rab5 is required in metastatic cancer cells for Caveolin-1-enhanced Rac1 activation, migration and invasion, J. Cell Sci. 127 (Pt 11) (2014) 2401–2406, https://doi.org/10.1242/jcs.141689.
[45] T.B. Dorff, et al., Randomized Phase II Trial of Abiraterone Alone or With Dasatinib in Men With Metastatic Castration-resistant Prostate Cancer (mCRPC), Clinical Genitourinary Cancer 17 (4) (2019) 241–247.e1, https://doi.org/10.1016/j.clgc.2019.02.010.
[46] F.G. Quest, A., et al., The Caveolin-1 Connection to Cell Death and Survival, Curr. Mol. Med. 13 (2) (2013) 266–281, https://doi.org/10.2174/156652413804810745.
[47] J.G. Fernández, et al., Survivin expression promotes VEGF-induced tumor angiogenesis via PI3K/Akt enhanced β-catenin/Tcf-Lef dependent transcription, Molecular Cancer 13 (2014) 1–15, https://doi.org/10.1186/1476-4598-13-209.
[48] I. Garmendia, et al., YES1 drives lung cancer growth and progression and predicts sensitivity to dasatinib, Am. J. Respir. Crit. Care Med. 200 (7) (2019) 888–899, https://doi.org/10.1164/rccm.201807-1292oc.
[49] J.R. Glenney, Tyrosine phosphorylation of a 22-kDa protein is correlated with transformation by Rous sarcoma virus, J. Biol. Chem. 264 (34) (1989) 20163–20166.
[50] E. Goicovich, et al., Enhanced degradation of proteins of the basal lamina and stroma by matrix metalloproteinases from the salivary glands of Sjögren's syndrome patients: Correlation with reduced structural integrity of acini and ducts, Arthritis Rheum. 48 (9) (2003) 2573–2584, https://doi.org/10.1002/art.11178.
[51] S. Guerrero, et al., Gold nanoparticles as tracking devices to shed light on the role of caveolin-1 in early stages of melanoma metastasis, Nanomedicine 13 (12) (2018) 1447–1462, https://doi.org/10.2217/nnm-2017-0390.
[52] J.F. Hainfeld, et al., In Vivo Vascular Casting, Microsc. Microanal. 11 (Suppl 2) (2005) 1216–1217, https://doi.org/10.1017/s143192760550847x.
[53] J.H. Hanke, et al., Discovery of a novel, potent, and Src family-selective tyrosine kinase inhibitor: Study of Lck- and FynT-dependent T cell activation, J. Biol. Chem. 271 (2) (1996) 695–701, https://doi.org/10.1074/jbc.271.2.695.
[54] Y.G. Ko, et al., Early effects of PP60(v-src) kinase activation on caveolae, J. Cell. Biochem. 71 (4) (1998) 524–535, https://doi.org/10.1002/(SICI)1097-4644(19981215)71:4<524::AID-JCB7>3.0.CO;2-B.
[55] L. Labrecque, et al., Src-mediated tyrosine phosphorylation of caveolin-1 induces its association with membrane type 1 matrix metalloproteinase, J. Biol. Chem. 279 (50) (2004) 52132–52140, https://doi.org/10.1074/jbc.M409617200.
[56] H. Lee, et al., Constitutive and growth factor-regulated phosphorylation of caveolin-1 occurs at the same site (Tyr-14) in vivo: Identification of a c-Src/Cav-1/Grb7 signaling cassette, Mol. Endocrinol. 14 (11) (2000) 1750–1775, https://doi.org/10.1210/mend.14.11.0553.
[57] L. Lobos-Gonzalez, et al., Caveolin-1 is a risk factor for postsurgery metastasis in preclinical melanoma models, Melanoma Res. 24 (2) (2014) 108–119, https://doi.org/10.1097/CMR.0000000000000046.
[58] C.C. Mastick, et al., Caveolin-1 and a 29-kDa caveolin-associated protein are phosphorylated on tyrosine in cells expressing a temperature-sensitive v-Abl kinase, Exp. Cell Res. 266 (1) (2001) 142–154, https://doi.org/10.1006/excr.2001.5205.
[59] C.C. Mastick, M.J. Brady, A.R. Saltiel, Insulin stimulates the tyrosine phosphorylation of caveolin, J. Cell Biol. 129 (6) (1995) 1523–1531, https://doi.org/10.1083/jcb.129.6.1523.
[60] C.C. Mastick, A.R. Saltiel, Insulin-stimulated tyrosine phosphorylation of caveolin is specific for the differentiated adipocyte phenotype in 3T3-L1 cells, J. Biol. Chem. 272 (33) (1997) 20706–20714, https://doi.org/10.1074/jbc.272.33.20706.
[61] F. Meng, et al., The phospho-caveolin-1 scaffolding domain dampens force fluctuations in focal adhesions and promotes cancer cell migration, Mol. Biol. Cell 28 (16) (2017) 2190–2201, https://doi.org/10.1091/mbc.E17-05-0278.
[62] W.A. Messersmith, et al., Efficacy and pharmacodynamic effects of bosutinib (SKI-606), a Src/Abl inhibitor, in freshly generated human pancreas cancer xenografts, Mol. Cancer Ther. 8 (6) (2009) 1484–1493, https://doi.org/10.1158/1535-7163.MCT-09-0075.
[63] N.B. Mettu, et al., A phase I study of gemcitabine + dasatinib (gd) or gemcitabine + dasatinib + cetuximab (GDC) in refractory solid tumors, Cancer Chemother. Pharmacol. 83 (6) (2019) 1025–1035, https://doi.org/10.1007/s00280-019-03805-6.
[64] F. Musumeci, et al., An update on dual Src/Abl inhibitors, Future Med. Chem. 4 (6) (2012) 799–822, https://doi.org/10.4155/fmc.12.29.
[65] S. Nam, et al., Action of the Src family kinase inhibitor, dasatinib (BMS-354825), on human prostate cancer cells, Cancer Res. 65 (20) (2005) 9185–9189, https://doi.org/10.1158/0008-5472.CAN-05-1731.
[66] M. Nethe, P.L. Hordijk, A model for phospho-caveolin-1-driven turnover of focal

adhesions, Cell Adhes. Migration 5 (1) (2011) 59–64, https://doi.org/10.4161/cam.5.1.13702.
[67] R. Nomura, T. Fujimoto, Tyrosine-phosphorylated caveolin-1: Immunolocalization and molecular characterization, Mol. Biol. Cell 10 (4) (1999) 975–986, https://doi.org/10.1091/mbc.10.4.975.
[68] M.O. Parat, B. Anand-Apte, P.L. Fox, Differential caveolin-1 polarization in endothelial cells during migration in two and three dimensions, Mol. Biol. Cell 14 (8) (2003) 3156–3168, https://doi.org/10.1091/mbc.E02-11-0761.
[69] M. Patarroyo, K. Tryggvason, I. Virtanen, Laminin isoforms in tumor invasion, angiogenesis and metastasis, Semin. Cancer Biol. 12 (3) (2002) 197–207, https://doi.org/10.1016/S1044-579X(02)00023-8.
[70] M.A. del Pozo, et al., Phospho-caveolin-1 mediates integrin-regulated membrane domain internalization, Nat. Cell Biol. 7 (9) (2005) 901–908, https://doi.org/10.1038/ncb1293.
[71] A. Puyraimond, et al., MMP-2 colocalizes with caveolae on the surface of endothelial cells, Exp. Cell Res. 262 (1) (2001) 28–36, https://doi.org/10.1006/excr.2000.5069.
[72] M. Sáinz-Jaspeado, et al., Caveolin-1 modulates the ability of Ewing's sarcoma to metastasize, Mol. Cancer Res. 8 (11) (2010) 1489–1500, https://doi.org/10.1158/1541-7786.MCR-10-0060.
[73] M.P. Sánchez-Bailón, et al., Src kinases catalytic activity regulates proliferation, migration and invasiveness of MDA-MB-231 breast cancer cells, Cell. Signal. 24 (6) (2012) 1276–1286, https://doi.org/10.1016/j.cellsig.2012.02.011.
[74] M.M. Schittenhelm, et al., Dasatinib (BMS-354825), a dual SRC/ABL kinase inhibitor, inhibits the kinase activity of wild-type, juxtamembrane, and activation loop mutant KIT isoforms associated with human malignancies, Cancer Res. 66 (1) (2006) 473–481, https://doi.org/10.1158/0008-5472.CAN-05-2050.
[75] A.J. Scott, et al., Evaluation of the efficacy of dasatinib, a Src/Abl inhibitor, in colorectal cancer cell lines and explant mouse model, PLoS ONE 12 (11) (2017) p : e0187173. 10.1371/journal.pone.0187173.
[76] S. Thomas, et al., Src and caveolin-1 reciprocally regulate metastasis via a common downstream signaling pathway in bladder cancer, Cancer Res. 71 (3) (2011) 832–841, https://doi.org/10.1158/0008-5472.CAN-10-0730.
[77] V.A. Torres, et al., Rab5 mediates caspase-8-promoted cell motility and metastasis, Mol. Biol. Cell 21 (2) (2010) 369–376, https://doi.org/10.1091/mbc.E09-09-0769.
[78] M. Ushio-Fukai, et al., Cholesterol depletion inhibits epidermal growth factor receptor transactivation by angiotensin II in vascular smooth muscle cells: Role of cholesterol-rich microdomains and focal adhesions in angiotensin II signaling, J. Biol. Chem. 276 (51) (2001) 48269–48275, https://doi.org/10.1074/jbc.M105901200.
[79][79] H. Yamaguchi, et al., Lipid rafts and caveolin-1 are required for invadopodia formation and extracellular matrix degradation by human breast cancer cells, Cancer Res. 69 (22) (2009) 8594–8602, https://doi.org/10.1158/0008-5472.CAN-09-2305.
[80] S.K. Akiyama, K. Olden, K.M. Yamada, Fibronectin and integrins in invasion and metastasis, Cancer Metastasis Rev. 14 (3) (1995) 173–189, https://doi.org/10.1007/BF00690290.